Journal of Fluorescence (2024) 34:2783–2791
https://doi.org/10.1007/s10895-023-03484-w

RESEARCH

Synthesis, Crystal Structure and Fluorimetric Study of 2-phenylphthalazin-1(2H)-one: a Highly Selective Florescent Chemosensor for Detection of Fe^{3+} and Fe^{2+} Metal Ions

Shahzad Sharif[1] · Muhammad Shahbaz[1] · Onur Şahin[2] · Muhammad Aqib Khurshid[1] · Maryam Musaffa Anbar[1] · Birra Dar[1]

Received: 16 September 2023 / Accepted: 20 October 2023 / Published online: 1 November 2023

Abstract

A ligand, 2-phenylphthalazin-1(2H)-one (**K**), was synthesized by refluxing 2-formylbenzoic acid with phenyl hydrazine in presence of ethanol. FTIR, elemental analysis and single crystal XRD techniques were used to elucidate the structure. Fluorimetric turn-off response was recorded when solution of ligand (**K**) in DMF was treated with aqueous solution of Fe^{3+} and Fe^{2+} metal ions. No specific changes were observed on addition of other metal ions (Pb^{2+}, Cd^{2+}, Mn^{2+}, Zn^{2+}, Ba^{2+}, Ni^{2+}, Al^{3+}, Ag^{1+}, Co^{2+}, Ca^{2+}, Cu^{2+}, Mg^{2+}, Cr^{3+}). Limit of Detection (LOD) was calculated for Fe^{2} and Fe^{3+}as 2.4 µM and 2.5µM respectively, which is quite below to the recommended value 5.4 µM of the Environment Protection Agency of USA. Association constants for Fe^{3+} and Fe^{2+} metal ions were determined as 6×10^{-4} M^{-1} and 3.6×10^{-4} M^{-1} respectively. Benesi-Hildebrand plot confirmed 1:1 binding ratio between metal ions and ligand.

Keywords Schiff base · Single XRD · Chemosensor · Turn off fluorescence · Fe^{3+} and Fe^{2+}

Introduction

Ground water located in the industrial area contains high level of heavy metal ions. These metal ions contaminate water bodies and deposit into the plants and animals. These deposited heavy metal ions introduce to the human body when they consumed water, plants or animals and cause health issues in human beings [1].

Iron is included among the most essential metal ions that exist in the human body and take part in different physiological processes. It is most abundant metal ion present in both combined and free state in human body. According to the Environmental Protection Agency of United States maximum concentration of Fe ions in the water should be 5.37 µM [2]. It involves in the biological and chemical reactions occur in the body [3]. There is a list of body tissues like liver, spleen, and kidneys etc. that contain iron metal ions. About 60 to 70% of iron in the human body is present in the hemoglobin that helps in the transportation of oxygen to the each and every cell of human body. Iron exists in both Fe^{2+} and Fe^{3+}oxidation states [4]. Iron is an important element that play role in many biochemical processes. For example, it not only helps hemoglobin for the transport of oxygen to the tissues and carbon dioxide out of the tissues but take part in the storage of oxygen in the muscle tissues [5]. It catalyzes several reactions of enzymes related to oxygen, take part in the synthesis of nucleic acids, some enzymes like cytochromes, hydrogenases etc. use iron as cofactor [6]. It takes part in cellular metabolism, oxidation reactions [7], mitochondrial respiration and electron transfer Fig. 1. Its presence in the hairs and blood make it important for the forensic investigation. Imbalance in the concentration of iron in human body effects human health badly. Human body absorb Fe^{3+} ions through intestine when it is present in its low oxidation state [8]. Imbalance in the amount of Fe^{3+} ions in the body occurs when these metal ions are taken from external environment in excess. It increases the chance of infectious diseases [9]. High and low level of Fe^{3+} ions concentration causes heart and liver diseases and it is also responsible for some neurological disorders [10]. Deficiency of Fe^{3+} ions cause

✉ Shahzad Sharif
mssharif@gcu.edu.pk

[1] Materials Chemistry Laboratory, Department of Chemistry, Govt. College University, Lahore 54000, Pakistan

[2] Department of Occupat Health & Safety, Faculty of Health Sciences, Sinop University, TR-57000 Sinop, Turkey

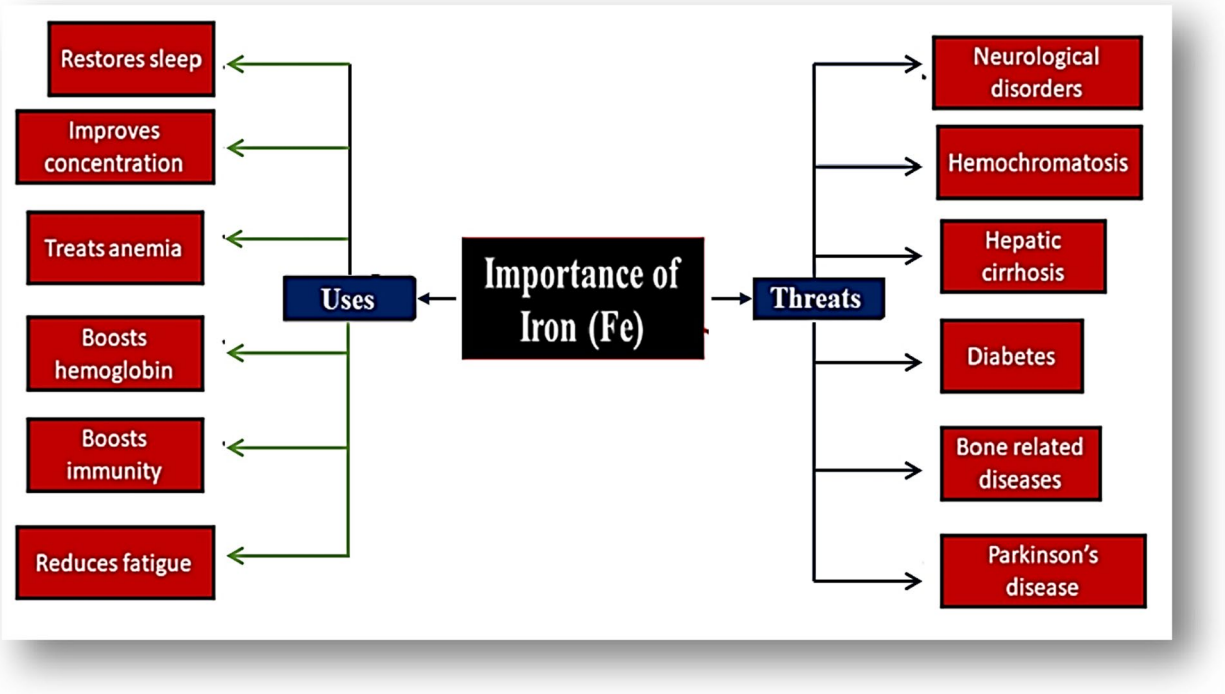

Fig. 1 Role of iron ions in human body

hemochromatosis, liver damage [11], Anemia [12], loss of motor neuron control, breathing problems, diabetes [13], hepatic cirrhosis [14], increases chance for cancer, decrease in the immunity, decrease in the liver development, heart diseases [15], and low blood pressure. Similarly, high level of Fe^{3+} ions is injurious to health and causes several human diseases. High level of metal ions reduces organ functions and causes the oxidation of cellular components that lead to the production of reactive oxygen species by Fenton reaction [16]. These reactive oxygen species damage cellular contents like proteins, DNA, RNA, and lipid that cause the cellular toxicity and leads to the neurological disorder [12]. Accumulation of Fe^{3+} ions damage kidneys and liver which result in hemochromatosis, hepatitis and bone related diseases. Elevated level of Fe^{3+}ions also cause Parkinson's disease, Alzheimer's disease and Huntington's disease [16]. Similar effects occur on the human body when amount of Fe^{2+} is imbalanced. Industrial revolution has created serious issues of water contamination for human beings. Industries release their untreated harmful waste materials directly into water resources that develop serious health issues for human beings and for their environment. These industrial wastes water contain heavy metals like Fe^{3+}, Fe^{2+},Cr^{3+}, Pb^{2+}, Hg^{2+}etc. that are potential threat to living organisms [17]. It increases the need to develop techniques for heavy metal detection in our environment. There is a variety of sophisticated analytical techniques for detection of metal ions such as flame atomic absorption spectroscopy (AAS) [18], HPLC, Inductively coupled plasma mass spectroscopy, atomic absorption spectroscopy [12], electrothermal atomization atomic absorption spectrometry (ETAAS) [5], voltammetry, ion pair chromatography and X-rays fluorescence. These methods are very effective but they are time consuming [8], requires expensive instrumentation and pretreatment of sample. Complex techniques are involved in these methods and trained professionals are required for their operation. These methods are not suitable for the on-site analysis of metal ions [19]. In the last few decades ligands have attracted attention of scientists due to their advantages over traditional analytical techniques for metal ions detection. Ligands have high sensitivity, low cost, easy to use[20], high selectivity and possess good resolution. These sensors are easy to handle and safe to use for immediate metal ions detection. Various mechanisms involved in the change of fluorescence intensity of ligand developed base for the analysis of metal ions by chemo sensors. These methods include fluorescence resonance energy transfer (FRET), intra-ligand charge transfer (ICT), photo-induced electron transfer (PET), excited state intramolecular proton transfer (PET) [21]. There are three expected behaviors of ligands upon interaction with metal ions. These behaviors include turn-on mode, turn-off mode and change in the emission wavelength which help in detection of various metal ions [22].

In this work, a ligand (**K**) was developed by reacting 2-formylbenzoic acid with phenyl hydrazine dissolved in ethanol. Crystallographic study and photometric properties

of ligand (**K**) have been studied extensively. The ligand showed significantly turn-off behavior for Fe^{3+} and Fe^{2+} metal ions in aqueous media without maintaining pH by using buffer. LOD, LOQ, binding constant and Stern Volmer constant were studied at length. It can be concluded that ligand (**K**) is very effective for the qualitative and quantitative detection of iron ions.

Experimental

Chemical and Reagents

All chemicals were obtained commercially from Sigma Aldrich/Alfa Aesar and used for the synthesis of ligand (**K**). Analytical grade solvents were also used throughout the experiment. Distilled water, precursor compounds (2-formylbenzoic acid and phenyl hydrazine; 97% purity), nitrates, chlorides and sulfate salts of metal ions ($FeCl_3$, $FeSO_4$, Pb $(NO_3)_2$, $CdCl_2$, $MnSO_4$, $ZnSO_4$, $BaCl_2$, $NiCl_2$, $AlCl_3$, $AgNO_3$, $CoSO_4$, $CaCl_2$, $CuSO_4$, $MgCl_2$, $CrCl_3$) were used without further purification.

Equipment

Elmasonic (sonicator) was used to homogenize solution of the ligand and metal ions. TLC (Thin Layered Chromatography) using silica gel plates 60 F254 were used to monitor the progress of the reaction. The percentage detection of N, C and N was performed on the Elemental Analyzer, Vario Micro Cube (Elementar, Germany). Fourier transform infrared spectrum was measured using ATR sample compartment on Bruker Tensor-27 spectrophotometer (Billerica, MA, USA) in the range of 400–4000 cm^{-1}. The spectrofluorometric readings were taken by spectrophotometer (Agilent Cary Eclipse Fluorescence Spectrophotometer).

Synthesis and Characterization of 2-phenylphthalazin-1(2H)-one (K)

Ethanolic solutions (10 ml) of 2-formylbenzoic acid (1 mmol) and phenyl hydrazine (1 mmol) were prepared separately and transferred into the round bottom flask. After refluxing the reaction mixture for 8 h at 70 °C, TLC was employed to check the progress of the reaction. After completion of reaction, yellowish colored precipitates were separated by filtration. The product was washed with distilled water and air dried. The product was dissolved in DMF/Ethanol to obtain yellowish block-colored crystals after 5 days, Melting point: 300 °C. IR (KBr cm^{-1}): 1708 (C=O), 1619 (C=N). Analysis (%) Calc. for $C_{14}H_{10}N_2O$ (222.24): N, 12.60; C, 75.59; H, 4.50; Found: N, 12.42; C, 75.37; H, 4.61. Yield ca. 76%.

Suitable crystal of **K** was mounted on a Bruker diffractometer equipped with a graphite-monochromatic Mo-Karadiation at 296 K. The structure was solved by direct methods using SHELXS-2013 [23] and refined by full-matrix least-squares methods on F^2using SHELXL-2013 [24]. All non-hydrogen atoms were refined with anisotropic parameters using Bruker APEX2 [25] data collection, MERCURY programs [26] program for molecular graphics and WinGX [27] to prepare material for publication. Details of data collection for crystal structure determinations are presented in table S1 & S2† and molecular structure of ligand **K** is shown in Fig. 2.

Preparation of the Ligand Solution and Metal Ions Standard Solutions

The ligand **K** was dissolved in DMF to make solution with concentration of 10^{-4} M. Similarly, 10^{-4} M solutions were also prepared by dissolving nitrates, chlorides and sulfate salts of different metal ions ($FeCl_3$, $FeSO_4$, $Pb(NO_3)_2$, $CdCl_2$, $MnSO_4$, $ZnSO_4$, $BaCl_2$, $NiCl_2$, $AlCl_3$, $AgNO_3$, $CoSO_4$, $CaCl_2$, $CuSO_4$, $MgCl_2$, $CrCl_3$) in distilled water.

Results and Discussions

Presence of heaving metals ions (micro-molar range) in aquatic ecosystems causes severe health issues. In coordination chemistry, Schiff bases are extensively used in bioinorganic chemistry due to their capability of making stable complexes. They possess good electron-donating group which renders its applications to chemical sensing in detection of metal ions by coordinating electron pair. The ligand 2-phenylphthalazin-1(2H)-one (**K**) was synthesized conveniently (Scheme 1). Characterization was performed with the help of FTIR, elemental analysis and XRD analysis which confirmed the product (Fig. 2). Strong bands of FTIR spectrum at 1708 and 1619 cm^{1-} corresponds to C=C and

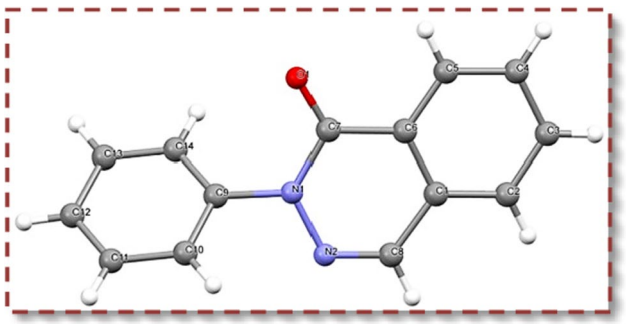

Fig. 2 Molecular structure of ligand **K**

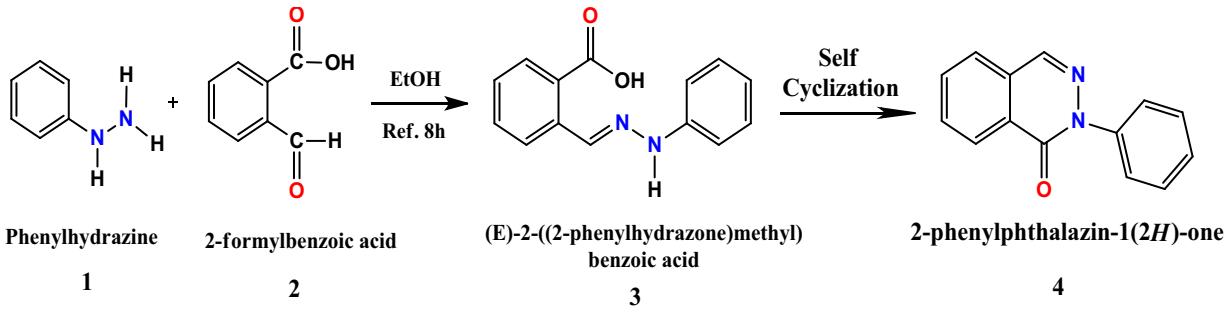

Scheme 1 Synthesis of 2-phenylphthalazin-1(2H)-one (**K**)

C = N stretching vibrations. The ligand (**K**) showed fluorescence quenching response towards Fe^{3+} and Fe^{2+} ions.

Spectrofluorometric Study of 2-phenylphthalazin-1(2H)-one (K)

Standard solution of the sensor (10^{-4}M) was prepared in DMF. Different metal ions were dissolved in distilled water to get 10^{-4} M salt solutions without adding any buffer to maintain pH. Fluorescence study revealed that the ligand (**K**) produced a very strong emission band at 431nm after excitation at 372nm wavelength (Fig. S1†). Addition of various metal ions (Fe^{3+}, Fe^{2+}, Pb^{2+}, Cd^{2+}, Mn^{2+}, Zn^{2+}, Ba^{2+}, Ni^{2+}, Al^{3+}, Ag^{1+}, Co^{2+}, Ca^{2+}, Cu^{2+}, Mg^{2+}, Cr^{3+}) to the separate solution of ligand (**K**) did not produce any prominent change in the emission intensity except Fe^{3+} ion and Fe^{2+} ions which quenched emission band at 431nm (Fig. 3A), bar graph showing quenching is shown in Fig. 3B. It indicated the possible use of ligand (**K**) for the selective detection of Fe^{3+} ion and Fe^{2+} ions in aqueous system.

With the increase in concentration of Fe^{3+} and Fe^{2+} ions to the solution of ligand **K** decrease the intensity of the ligand. Fe^{2+} ions caused 67.07% quenching in the intensity of the ligand whereas 81.05% decrease was noted with Fe^{3+} ions up to 10 equivalents. Stern–Volmer constant was calculated to study quenching extent of Fe^{3+} and Fe^{2+} ions. The higher value of Stern–Volmer constant the stronger is the quenching of ligand intensity by metal ions.

Calculation of Limit of Detection (LOD) and Limit of Quantification (LOQ)

For fluorescence titration, stock solution of ligand (**K**) and metal ions were prepared. After adding solution of metal ions, the ligand solution was stirred properly for few seconds before taking fluorescence spectra. Fluorescence intensity of ligand (**K**) was quenched by gradual increase in the concentration of Fe^{3+} and Fe^{2+} metal ions (Fig. 4A & C). LOD and LOQ are important characteristics of a fluorescence ligand. Graphs of Fe^{3+} and Fe^{2+} metal ions between intensity "I" of the ligand against concentration of Iron metal ions was plotted as shown in Fig. 4B and C. Following equations were used for the calculations of Limit of Detection (LOD) and Limit of Quantification (LOQ) [28].

The SD intercept and slope taken from the graph and were used to calculate LOD and LOQ. Fe^{3+} and Fe^{2+} ions showed limit of detection calculated as 2.5 µM and 2.4 µM respectively. Similarly, limit of quantification came out to be 7.7 µM and 7.2 µM for both metal ions. Table 1 shows comparison of limit of detection of some ligands for Fe^{3+} and Fe^{2+} ions reported in the literature.

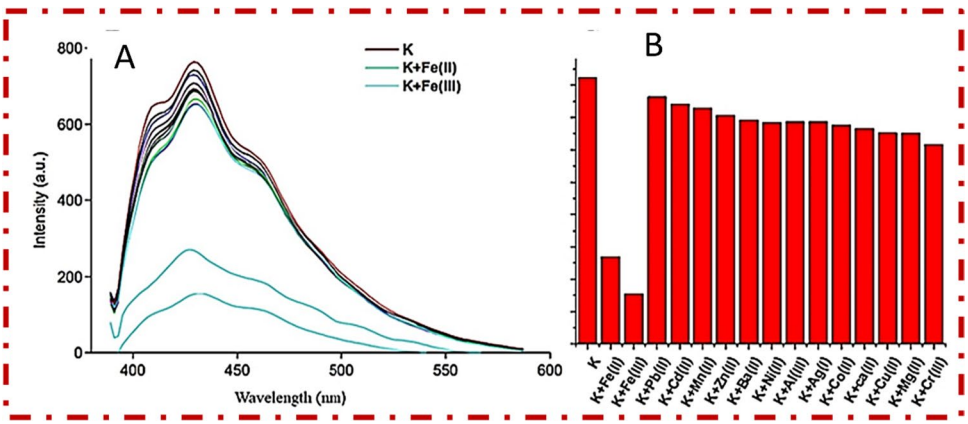

Fig. 3 (**A**) Emission spectra of ligand **K** with different metal ions. (**B**) Bar graph of ligand **K** with different metal ions

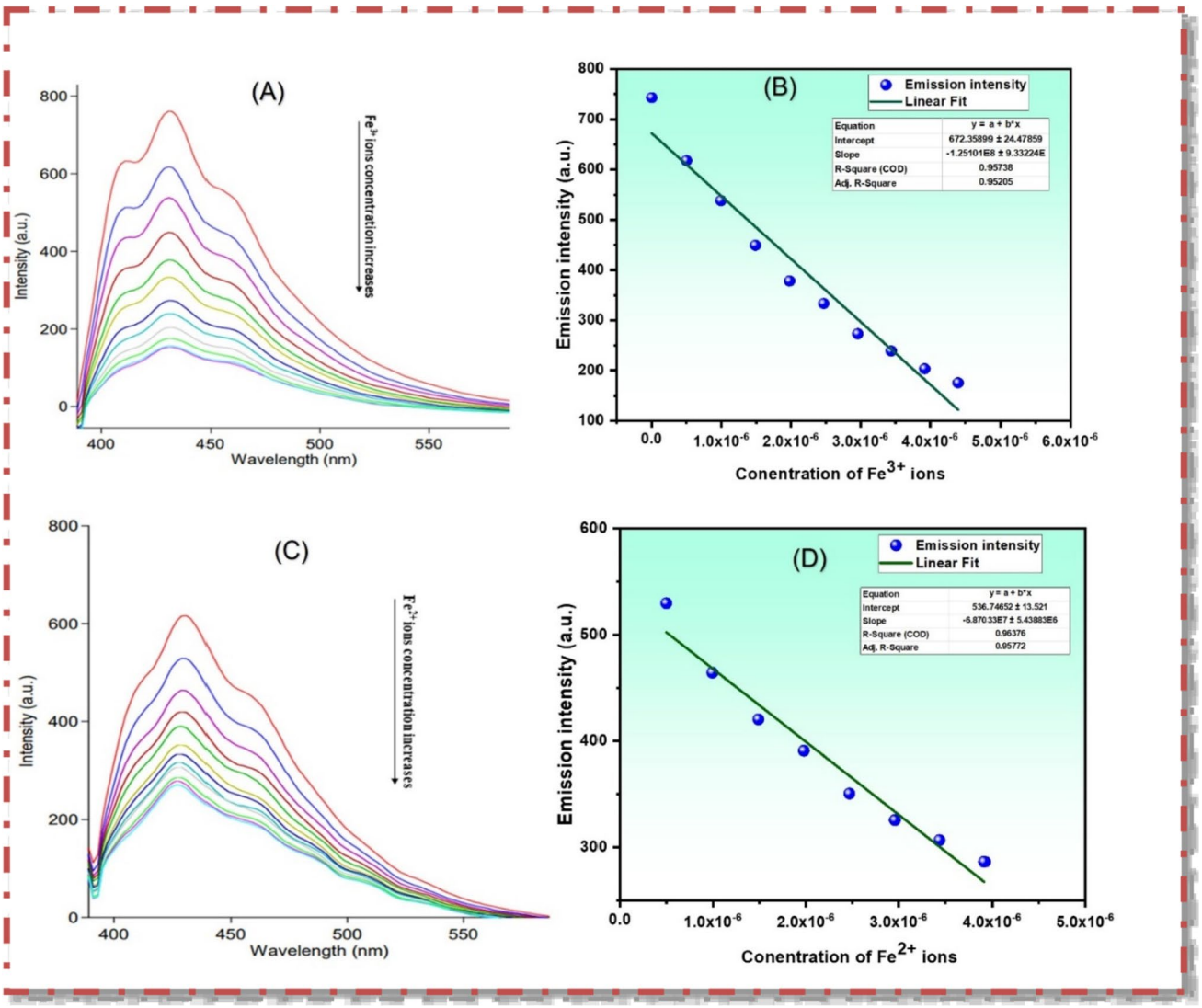

Fig. 4 (**A**) Fluorescence titration graph of ligand **K** with Fe^{3+} ions. (**B**) Fluorescence quenching graph of ligand **K** in the presence of Fe^{3+} ions. (**C**) Titration graph of ligand **K** with Fe^{2+} ions (**D**) Fluorescence quenching graph of ligand in the presence of Fe^{2+} ions

Stern–volmer Plot and Benesi–hildebrand Plot

Quenching is the process in which the fluorescence intensity of the compound is reduced by addition of certain substance (quencher). Dynamic quenching and static quenching are the two different quenching patterns. Dynamic quenching or collisional quenching is the result of interaction of quencher and excited state fluorophore due to which the fluorophore is deactivated to the ground state with no radiation. However, in static quenching, molecules form a non-fluorescent complex in ground state [9].

Emission intensity of the ligand (**K**) quenched at various concentration Fe^{3+} and Fe^{2+} metal ions which was studies by Stern–Volmer plot by using following equation:

$$\frac{\mathbf{Io}}{\mathbf{I}} = 1 + \mathbf{Ksv}[\mathbf{Q}] \tag{3}$$

'I_o' and 'I' are emission intensities in presence and absence of metal ions. [Q] is the concentration of metal ions whereas K_{sv} represents Stern–Volmer quenching constant. When all the variables are held constant, higher value of K_{sv} represents lower concentration of metal ions responsible for quenching. If stable complex is formed between cation and sensor, the proposed mechanism of complex formation is photo-induced electron transfer (PET) and type thereof is static quenching. In PET process, HOMO and LUMO of the ligand and the LUMO of the metal ions involves in the complex formation as shown in Fig. 5.

Table1 Comparison with other report ligands for detection of Fe^{3+} and Fe^{2+} ions

Fluorescent chemosensor	LOD (uM)	Ref
(E)-2-((pyren-1-ylmethylene)amino) benzenethiol	0.3 ppm (Fe^{3+})	[29]
((E)-2-((4-(diethylamino)benzylidene)amino)benzoic acid, (DBAB)	2.17 (Fe^{3+}) 2.06 (Fe^{2+})	[30]
2,5,7-Triarylimidazopyridine Scaffold	55.0 (Fe^{2+}) 36.64 (Fe^{3+})	[31]
Fluorescent probe based on N-oxide	0.21 (Fe^{2+})	[32]
Tween® 80 Quantum Dots	6.5 (Fe^{2+}) 2.5 (Fe^{3+})	[33]
(E)-N-(naphthalene-1-ylmethylene)pyridine-2- amine	0.15 (Fe^{2+})	[34]
N-aryl-O-acylhydroxylamine based probe	0.5 (Fe^{2+})	[35]
A conjugated microporous organic polymer (TPA-Bp)	5.37 (Fe^{2+}) 0.10 (Fe^{3+})	[36]
Furo [3,2-c] coumarin derivative	1.93 (Fe^{2+})	[37]
Rhodamine 6G dyes derivative	0.041 (Fe^{2+})	[38]
Phenylene–acetylene based sensor	0.02 (Fe^{2+})	[39]
NT-Fe Probe	0.089 (Fe^{2+})	[40]
ICT-based two photon and NIR fluorescent probe	4.5 (Fe^{2+})	[41]
Ligand DALD	1.3 (Fe^{2+}) 0.69 (Fe^{3+})	[42]
BODIPY-based fluorescent probe	0.292 (Fe^{2+})	[43]
A turn-on fluorescent probe $P_{Fe(II)}$	1.03 (Fe^{2+})	[44]
2−hydroxy−1−naphthaldehyde based probe	0.0363 (Fe^{2+})	[45]
2-phenylphthalazin-1(2H)-one (K)	2.5 (Fe^{3+}) 7.7 (Fe^{2+})	**Present Work**

If the LUMO of cation falls between the HOMO and LUMO of the ligand or fluorophore, the binding results into non-radiative path in which energy is dissipated.

The graph was plotted between I_o/I and [Q] for the analysis of quenching performance of Fe^{3+} and Fe^{2+} metal ions which showed linear relationship with corresponding regression coefficient (R^2). It indicated the formation of non-fluorescence ligand–metal complex in the ground state. The mechanism and type of quenching by the quencher in this case is photo-induced electron transfer (PET) and static quenching, respectively. Stern–Volmer constants for Fe^{3+} and Fe^{2+} ions obtained from graph were 8.70×10^4 M^{-1} and 2.71×10^4 M^{-1} that revealed good quenching efficiency of Fe^{3+} and Fe^{2+} ions towards ligand (**K**) (Fig. 6A & B).

Benesi-Hildebrand equation helps in determination of association constant (K_a) and binding stoichiometry as shown in Fig. 6C & D.

It was analyzed by changing the concentration of Fe^{3+} ions to see the impact on the ligand fluorescence intensity. 1:1 binding association of metal and ligand shows linearity according to the Benesi-Hildebrand equation (Eq. 4).

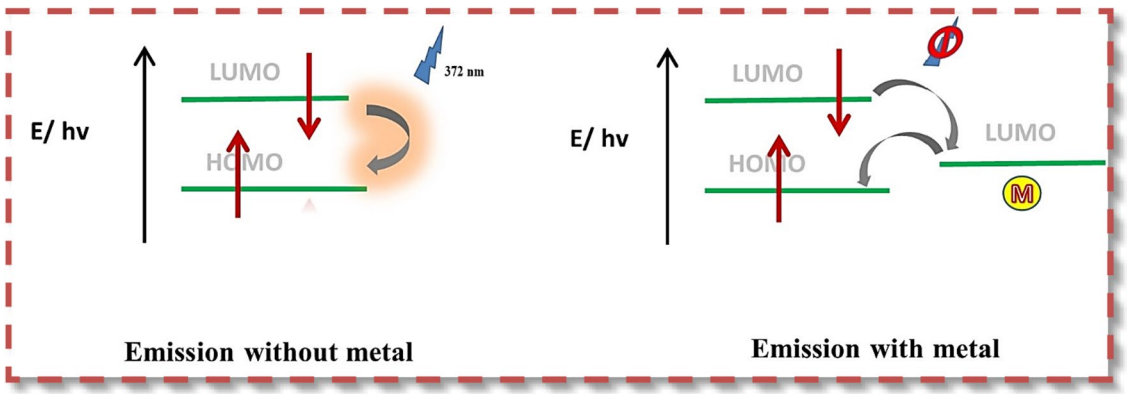

Fig. 5 Photo-induced electron transfer (PET) mechanism

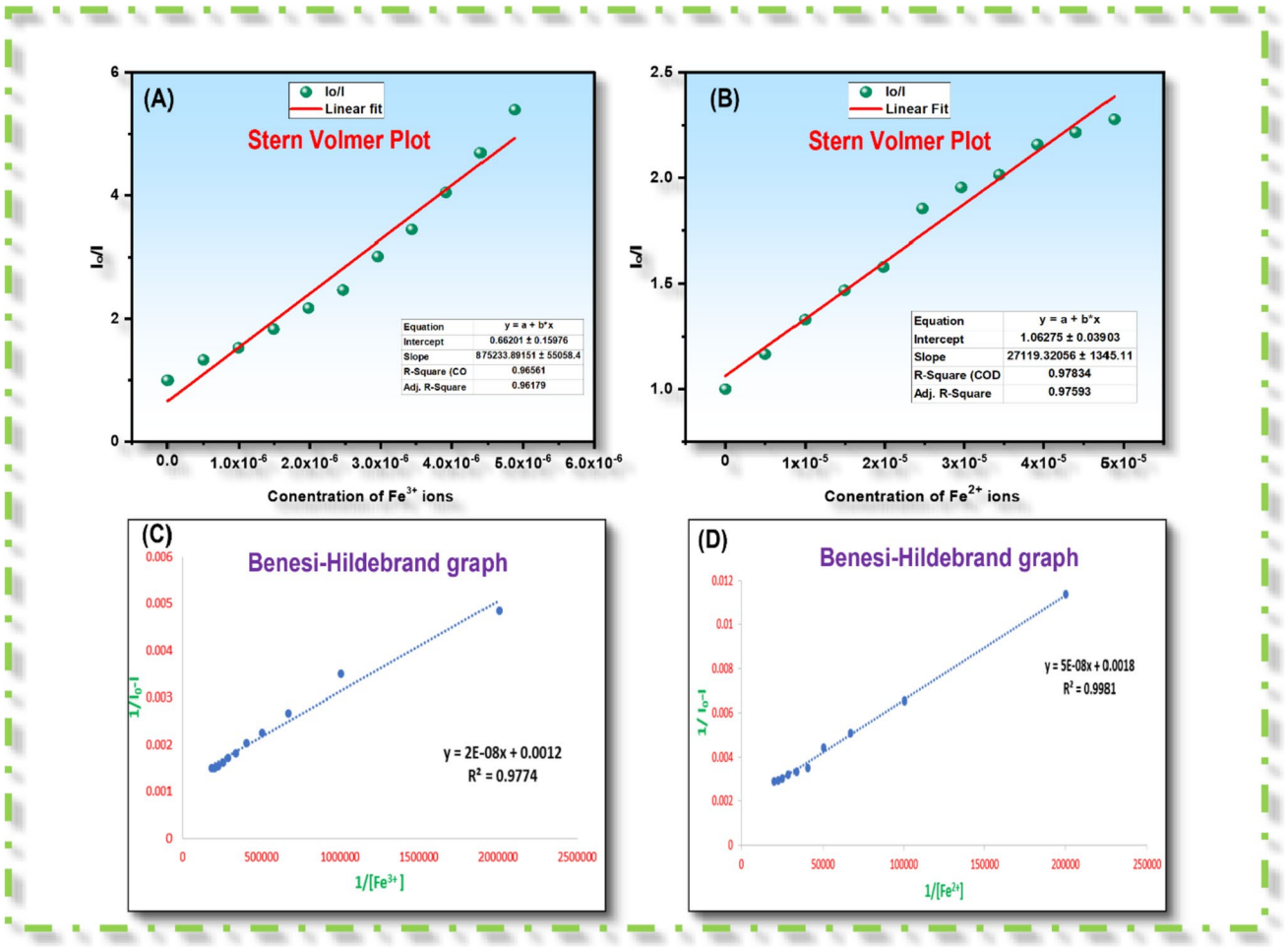

Fig. 6 (**A**) Stern–Volmer plot in presence of Fe^{3+} ions and (**B**) Fe^{2+} ions. (**C**) Benesi–Hildebrand plot for determination of association constant (Ka) of Fe^{3+} ions and (**D**) Fe^{2+} ions

$$\frac{1}{I - Io} = \frac{1}{Ka(Io - Imin)Q} + \frac{1}{Io - Imin} \tag{4}$$

"I_o" is the fluorescence intensity of ligand without metal ions. "I" is fluorescence intensity of ligand after the addition of Fe^{3+} and Fe^{2+} metal ions. "I_{min}" is the minimum intensity after the addition of metal ions. [Q] is the concentration of metal ions and "K_a" is association constant of ligand with metal ions. The graph was plot between $1/(I\text{-}I_o)$ and 1/[Q] to find out the association constant and apparent binding stoichiometry. Double reciprocal graph between $1/(I\text{-}I_o)$ and 1/[Q] showed linearity which confirmed 1:1 binding ratio between ligand and metal complex. Slope and intercept in the graph were used to find out K_a. The value of K_a for Fe^{3+} and Fe^{2+} ions were calculated as 6×10^4 M^{-1} and 3.6×10^4 M^{-1} respectively.

Conclusions and Future Perspective

In this work, we synthesized a new Schiff base derivative 2-phenylphthalazin-1(2H)-one (**K**) as fluorescent ligand for recognition and quantification of Fe^{3+} and Fe^{2+} ions. Amongst various metal ions, the ligand showed high selectivity and sensitivity towards Fe^{3+} and Fe^{2+} metal ions in aqueous environment by remarkable quenching effect. The ligand bound with Fe^{3+} and Fe^{2+} metal ions in 1:1 stoichiometric ratio and detected the metal concentration as low as 2.5 μM and 2.4 μM respectively which is lower than the recommended value of EPA US (5.4 μM). Association constants for ligand and metal ions were determined as 8.70×10^4 M^{-1} and 2.71×10^4 M^{-1} for Fe^{3+} and Fe^{2+} metal ions. The synthesized ligand has advantage over the common reported ligands due to its rapid water testing for Fe^{3+}

and Fe^{2+} metal ions without using buffer to maintain pH of the solution. Ligand (**K**) can also be explored for quantification of Fe^{3+} and Fe^{2+} ions in biological fluids as well as can be fabricated as electrode to be used as electrochemical sensor for Fe^{3+} and Fe^{2+}.

Abbreviations (**K**): 2-phenylphthalazin-1(2H)-one; (AAS): flame atomic absorption spectroscopy; HPLC: Inductively coupled plasma mass spectroscopy, atomic absorption spectroscopy, electrothermal atomization atomic absorption spectrometry; ETAAS: electrothermal atomization atomic absorption spectrometry; FRET: fluorescence resonance energy transfer; ICT: intra- ligand charge transfer; PET: photo-induced electron transfer; PET: excited state intramolecular proton transfer; LOD: Limit of Detection; LOQ: and Limit of Quantification; EPAUS: Environment Protection Agency of United States of America

Supplementary Information The online version contains supplementary material available at https://doi.org/10.1007/s10895-023-03484-w.

Acknowledgements We gratefully acknowledge financial assistance from the Higher Education Commission of Pakistan, HEC-NRPU project no.20-17612/NRPU/R&D/HEC/2021 and GCU-ORIC Project no. No. 85/ORIC/23.

Author Contributions Shahzad Sharif: Conceptualization, Supervision, Project administration, review, editing. Muhammad Shahbaz: Design experimentation, writing original draft. Onur Şahin: Single XRD analysis, write up, Muhammad Aqib Khurshid: Methodology and write up. Maryam Musaffa Anbar: Experimental set up, sample preparation. Birra Dar: Luminescence experimentation.

Funding There was no funding to disclose.

Availability of Data and Materials Data will be made available on request.

Declarations

Ethical Approval Not applicable.

Competing Interests The authors declare no competing interests.

References:

1. Nawaz H, Tian W, Zhang J, Jia R, Chen Z, Zhang J (2018) Cellulose-Based Sensor Containing Phenanthroline for the Highly Selective and Rapid Detection of Fe 2+ Ions with Naked Eye and Fluorescent Dual Modes. ACS Appl Mater Interfaces 10(2):2114–2121. https://doi.org/10.1021/acsami.7b17342
2. Jo TG, Bok KH, Han J, Lim MH, Kim C (2017) Colorimetric Detection of Fe3+ and Fe2+ and Sequential Fluorescent Detection of Al3+ and Pyrophosphate by an Imidazole-Based Chemosensor in a near-Perfect Aqueous Solution. Dye Pigment 139:136–147. https://doi.org/10.1016/j.dyepig.2016.11.052
3. Darole RS, Christopher Leslee DB, Mukherjee A, Gonnade RG, Karuppannan S, Senthilkumar B (2020) Anthrone-spirolactam and Quinoline Hybrid Based Sensor for Selective Fluorescent Detection of Fe 3+ Ions. Appl Organomet Chem 34(10). https://doi.org/10.1002/aoc.5867.
4. Gong X, Zhang H, Jiang N, Wang L, Wang G (2019) Oxadiazole-Based 'on-off' Fluorescence Chemosensor for Rapid Recognition and Detection of Fe2+ and Fe3+ in Aqueous Solution and in Living Cells. Microchem J 145:435–443. https://doi.org/10.1016/j.microc.2018.11.011
5. Gong X, Ding X, Jiang N, Zhong T, Wang G (2020) Benzothiazole-Based Fluorescence Chemosensors for Rapid Recognition and "Turn-off" Fluorescence Detection of Fe3+ Ions in Aqueous Solution and in Living Cells. Microchem J 152:104351. https://doi.org/10.1016/j.microc.2019.104351
6. Harsha KG, Rao BA, Baggi TR, Prabhakar S, Rao VJ (2020) Thiophene-Phenylquinazoline Probe for Selective Ratiometric Fluorescence and Visual Detection of Fe(Iii) and Turn-off Fluorescence for I− and Its Applications. Photochem Photobiol Sci 19(12):1707–1716. https://doi.org/10.1039/d0pp00193g
7. Zuo Z, Song X, Guo D, Guo Z, Niu Q (2019) A Dual Responsive Colorimetric/Fluorescent Turn-on Sensor for Highly Selective, Sensitive and Fast Detection of Fe3+ Ions and Its Applications. J Photochem Photobiol A Chem 382:111876. https://doi.org/10.1016/j.jphotochem.2019.111876
8. Tümay SO, Irani-Nezhad MH, Khataee A (2021) Multi-Anthracene Containing Fluorescent Probe for Spectrofluorimetric Iron Determination in Environmental Water Samples. Spectrochim. Acta Part A Mol Biomol Spectrosc 248:119250. https://doi.org/10.1016/j.saa.2020.119250.
9. Wang D, Ma C, Zhou X, Long W, Liu M, Zhang X, Wei Y (2021) Self-Dispersible Fluorescent Probe with Aggregation-Induced Emission Feature for Sequence Detection of Fe3+ and Ca2+. Colloid Interface Sci Commun 40:100358. https://doi.org/10.1016/j.colcom.2020.100358
10. Hou L, Liu T, Gong Y, Li J, Deng C, Zhang C, Wang Y, Shuang S, Liang W (2020) A Turn-on Schiff Base Fluorescent Probe for the Exogenous and Endogenous Fe 3+ Ion Sensing and Bioimaging of Living Cells. New J Chem 44(45):19642–19649. https://doi.org/10.1039/D0NJ04315J
11. Yıldız M, Sahiner N (2021) Tannic Acid for Simple and Highly Selective Visual Detection of Iron (II) and (III) Ions from Different Aqueous Environments. Water, Air, Soil Pollut 232(5):201. https://doi.org/10.1007/s11270-021-05116-0
12. Sayed A, Othman IMM, Hamam M, Gomaa H, Gadallah MI, Mostfa MA, Ali HRH, Emran MY, Abdel-Hakim M, Mahross MH (2021) A Novel Fluorescent Sensor for Fast and Highly Selective Turn-off Detection of Fe3+ in Water and Pharmaceutical Samples Using Synthesized Azopyrazole-Benzenesulfonamide Derivative. J Mol Struct 1225:129175. https://doi.org/10.1016/j.molstruc.2020.129175
13. Tümay SO, Haddad Irani-nezhad M, Khataee A (2020) Design of Novel Anthracene-Based Fluorescence Sensor for Sensitive and Selective Determination of Iron in Real Samples. J Photochem Photobiol A Chem 402:112819. https://doi.org/10.1016/j.jphotochem.2020.112819
14. Pundi A, Chang C-J, Chen J, Hsieh S-R, Lee M-C (2021) A Chiral Carbazole Based Sensor for Sequential "on-off-on" Fluorescence Detection of Fe3+ and Tryptophan/Histidine. Sensors Actuators B Chem 328:129084. https://doi.org/10.1016/j.snb.2020.129084
15. Roy A, Das S, Sacher S, Mandal SK, Roy P (2019) A Rhodamine Based Biocompatible Chemosensor for Al 3+, Cr 3+ and Fe 3+ Ions: Extraordinary Fluorescence Enhancement and a Precursor for Future Chemosensors. Dalt Trans 48(47):17594–17604. https://doi.org/10.1039/C9DT03833G
16. Dhivya R, Gomathi A, Viswanathamurthi P (2019) Pyrene Based Fluorescent Turn-on Chemosensor for Sequential Detection of Fe3+ and Fe2+ Ions and Its Application in Live Cell Imaging. J Fluoresc 29(3):797–802. https://doi.org/10.1007/s10895-019-02392-2
17. Dey S, Kumar A, Mondal PK, Modi KM, Chopra D, Jain VK (2020) An Oxacalix[4]Arene Derived Dual Sensing Fluorescent Probe for the Detection of As Oxyanions in Aqueous Media. Dalt Trans 49(22):7459–7466. https://doi.org/10.1039/D0DT00452A

18. Kaur J, Sharma S, Mehta SK, Kansal SK (2020) Highly Photoluminescent and PH Sensitive Nitrogen Doped Carbon Dots (NCDs) as a Fluorescent Sensor for the Efficient Detection of Cr (VI) Ions in Aqueous Media. Spectrochim. Acta Part A Mol Biomol Spectrosc 227:117572. https://doi.org/10.1016/j.saa.2019.117572.
19. Sangsin S, Srivilai P, Tongraung P (2021) Colorimetric Detection of Cr3+ in Dietary Supplements Using a Smartphone Based on EDTA and Tannic Acid-Modified Silver Nanoparticles. Spectrochim. Acta Part A Mol Biomol Spectrosc 246:119050. https://doi.org/10.1016/j.saa.2020.119050.
20. Jiang T, Bian W, Kan J, Sun Y, Ding N, Li, W, Zhou J (2021) Sensitive and Rapid Detection of Cr3+ in Live Cells by a Red Turn-on Fluorescent Probe. Spectrochim. Acta Part A Mol Biomol Spectrosc 245:118903. https://doi.org/10.1016/j.saa.2020.118903.
21. Seenan S, Manickam S, Kulathu Iyer S (2021) A New Furan Based Fluorescent Chemosensor for the Recognition of Cr3+ Ion and Its Application in Real Sample Analysis. J Photochem Photobiol A Chem 418:113441. https://doi.org/10.1016/j.jphotochem.2021.113441
22. Pivetta T, Masuri S, Cabiddu MG, Caltagirone C, Pintus A, Massa M, Isaia F, Cadoni E (2019) A Novel Ratiometric and Turn-on Fluorescent Coumarin-Based Probe for Fe. New J Chem 43(30):12032–12041. https://doi.org/10.1039/C9NJ02044F
23. Sheldrick GM (2008) A Short History of SHELX. Acta Crystallographica, A (64):112–122. https://doi.org/10.1107/S0108767307043930
24. Sheldrick GM (2015) Acta Cryst C(71):3–8. https://doi.org/10.1107/S2053229614024218
25. Bruker (2013) APEX2, SAINT and SADABS. Bruker AXS Inc., Madison
26. Macrae CF, Bruno IJ, Chisholm JA, Edgington PR, McCabe P, Pidcock E, Rodriguez-Monge L, Taylor R, van de Streek J, Wood PA (2008) Mercury CSD 2.0 – New Features for the Visualization and Investigation of Crystal Structures. J Appl Crystallogr 41(2):466–470. https://doi.org/10.1107/S0021889807067908.
27. Farrugia LJ (2012) J Appl Cryst 45:849–854. https://doi.org/10.1107/S0021889812029111
28. Shahbaz M, Sharif S, Saeed M, Ashraf A, Rehman Afzal TT (2023) A Facile and Highly Selective Fluorimetric Chemosensor 1,2,4-Aminonaphthol Sulfonic Acid for Detection of Copper Ions in Aqueous Medium. J Lumin 263:120149. https://doi.org/10.1016/j.jlumin.2023.120149
29. Wan C-F, Chang Y-J, Chien C-Y, Sie Y-W, Hu C-H, Wu A-T (2016) A New Multifunctional Schiff Base as a Fluorescence Sensor for Fe2+ and F− Ions, and a Colorimetric Sensor for Fe3+. J Lumin 178:115–120. https://doi.org/10.1016/j.jlumin.2016.05.039
30. Zhu X, Duan Y, Li P, Fan H, Han T, Huang X (2019) A Highly Selective and Instantaneously Responsive Schiff Base Fluorescent Sensor for the "Turn-off" Detection of Iron Ions. Anal Methods 11(5):642–647. https://doi.org/10.1039/C8AY02526F
31. Sasan S, Chopra T, Gupta A, Tsering D, Kapoor KK, Parkesh R (2022) Fluorescence, "Turn-Off" and Colorimetric Sensor for Fe 2+, Fe 3+, and Cu 2+ Ions Based on a 2,5,7-Triarylimidazopyridine Scaffold. ACS Omega 7(13):11114–11125. https://doi.org/10.1021/acsomega.1c07193
32. Zeng X, Chen J, Yu S, Liu Z, Ma M (2022) A Highly Selective and Sensitive "Turn-on" Fluorescent Probe for Fe2+ and Its Applications. J Lumin 250:119069. https://doi.org/10.1016/j.jlumin.2022.119069
33. Siahcheshm P, Heiden P (2023) High Quantum Yield Carbon Quantum Dots as Selective Fluorescent Turn-off Probes for Dual Detection of Fe2+/Fe3+ Ions. J Photochem Photobiol A Chem 435:114284. https://doi.org/10.1016/j.jphotochem.2022.114284
34. Santhoshkumar S, Velmurugan K, Prabhu J, Radhakrishnan G, Nandhakumar R (2016) A Naphthalene Derived Schiff Base as a Selective Fluorescent Probe for Fe2+. Inorganica Chim Acta 439:1–7. https://doi.org/10.1016/j.ica.2015.09.030
35. Xuan W, Pan R, Wei Y, Cao Y, Li H, Liang F-S, Liu K-J, Wang W (2016) Reaction-Based, "Off–On" Fluorescent Probe Enabling Detection of Endogenous Labile Fe 2+ and Imaging of Zn 2+ -Induced Fe 2+ Flux in Living Cells and Elevated Fe 2+ in Ischemic Stroke. Bioconjug Chem 27(2):302–308. https://doi.org/10.1021/acs.bioconjchem.5b00259
36. Zhang C, Pan G, He Y (2022) Conjugated Microporous Organic Polymer as Fluorescent Chemosensor for Detection of Fe3+ and Fe2+ Ions with High Selectivity and Sensitivity. Talanta 236:122872. https://doi.org/10.1016/j.talanta.2021.122872
37. Sarih NM, Ciupa A, Moss S, Myers P, Slater AG, Abdullah Z, Tajuddin HA, Maher S (2020) Furo[3,2-c]Coumarin-Derived Fe3+ Selective Fluorescence Sensor: Synthesis, Fluorescence Study and Application to Water Analysis. Sci Rep 10(1):7421. https://doi.org/10.1038/s41598-020-63262-7
38. Qiao R, Xiong W-Z, Bai C-B, Liao J-X, Zhang L (2018) A Highly Selective Fluorescent Chemosensor for Fe (III) Based on Rhodamine 6G Dyes Derivative. Supramol Chem 30(11):911–917. https://doi.org/10.1080/10610278.2018.1467016
39. Zhang Y-Y, Chen X-Z, Liu X-Y, Wang M, Liu J-J, Gao G, Zhang X-Y, Sun R-Z, Hou S-C, Wang H-M (2018) A Highly Sensitive Multifunctional Sensor Based on Phenylene-Acetylene for Colorimetric Detection of Fe2+ and Ratiometric Fluorescent Detection of Cd2+ and Zn2+. Sensors Actuators B Chem 273:1077–1084. https://doi.org/10.1016/j.snb.2018.07.012
40. Zhang X, Chen Y, Cai X, Liu C, Jia P, Li Z, Zhu H, Yu Y, Wang K, Li X, Sheng W, Zhu B (2020) A Highly Sensitive Rapid-Response Fluorescent Probe for Specifically Tracking Endogenous Labile Fe2+ in Living Cells and Zebrafish. Dye Pigment 174:108065. https://doi.org/10.1016/j.dyepig.2019.108065
41. Yang X, Wang Y, Liu R, Zhang Y, Tang J, Yang E, Zhang D, Zhao Y, Ye Y (2019) A Novel ICT-Based Two Photon and NIR Fluorescent Probe for Labile Fe2+ Detection and Cell Imaging in Living Cells. Sensors Actuators B Chem 288:217–224. https://doi.org/10.1016/j.snb.2019.02.123
42. Parsaei-Khomami A, Badiei A, Ghavami ZS, Ghasemi JB (2022) A New Fluorescence Probe for Simultaneous Determination of Fe2+ and Fe3+ by Orthogonal Signal Correction-Principal Component Regression. J Mol Struct 1252:131978. https://doi.org/10.1016/j.molstruc.2021.131978
43. Xu W, Wu P, Li X, Liu S, Feng L, Xiong H (2021) Two Birds with One Stone: A Highly Sensitive near-Infrared BODIPY-Based Fluorescent Probe for the Simultaneous Detection of Fe2+ and H+ in Vivo. Talanta 233:122601. https://doi.org/10.1016/j.talanta.2021.122601
44. Khatun S, Biswas S, Binoy A, Podder A, Mishra N, Bhuniya S (2020) Highly Chemoselective Turn-on Fluorescent Probe for Ferrous (Fe2+) Ion Detection in Cosmetics and Live Cells. J Photochem Photobiol B Biol 209:111943. https://doi.org/10.1016/j.jphotobiol.2020.111943
45. Kouser R, Zehra S, Khan RA, Alsalme A, Arjmand F, Tabassum S (2021) "Turn–on" Benzophenone Based Fluorescence and Colorimetric Sensor for the Selective Detection of Fe2+ in Aqueous Media: Validation of Sensing Mechanism by Spectroscopic and Computational Studies. Spectrochim. Acta Part A Mol Biomol Spectrosc 247:119156. https://doi.org/10.1016/j.saa.2020.119156.